

Joint Communication and Control for Wireless Autonomous Vehicular Platoon Systems

Tengchan Zeng¹, Omid Semiari², Walid Saad¹, and Mehdi Bennis³

¹ Wireless@VT, Electrical and Computer Engineering Department, Virginia Tech, Blacksburg, VA, USA,
Emails: {tengchan, walids}@vt.edu.

² Department of Electrical and Computer Engineering, Georgia Southern University, Statesboro, GA, USA,
Email: osemiari@georgiasouthern.edu.

³ Centre for Wireless Communications, University of Oulu, Oulu, Finland, Email: bennis@ee.oulu.fi.

Abstract

Autonomous vehicular platoons will play an important role in improving on-road safety in tomorrow's smart cities. Vehicles in an autonomous platoon can exploit vehicle-to-vehicle (V2V) communications to collect information, such as velocity and acceleration, from surrounding vehicles so as to maintain the target velocity and inter-vehicle distance. However, due to the dynamic on-vehicle data processing rate and the uncertainty of the wireless channel, V2V communications within a platoon will experience a wireless system delay. Such system delay can impair the vehicles' ability to stabilize their speed and distances within their platoon. In this paper, the problem of joint communication and control system is studied for wirelessly connected autonomous vehicular platoons. In particular, a novel framework is proposed for optimizing a platoon's operation while jointly taking into account the delay of the wireless V2V network and the stability of the vehicle's control system. First, stability analysis for the control system is performed and the maximum wireless system delay requirements which can prevent the instability of the control system are derived. Then, delay analysis is conducted to determine the end-to-end delay, including queuing, processing, and transmission delay for the V2V link in the wireless network. Subsequently, using the derived wireless delay, a lower bound and an approximated expression of the reliability for the wireless system, defined as the probability that the wireless system meets the control system's delay needs, are derived. Then, the parameters of the control system are optimized in a way to maximize the derived wireless system reliability. Simulation results corroborate the analytical derivations and study the impact of parameters, such as the packet size and the platoon size, on the reliability performance of the vehicular platoon. More importantly, the simulation results shed light on the benefits of integrating control system and wireless network design while providing guidelines for designing an autonomous platoon so as to realize the required wireless network reliability and control system stability.

A preliminary version of this work appears in the proceeding of IEEE ICC, 2018 [1]. This research was supported by the U.S. National Science Foundation under Grants CNS-1513697, CNS-1739642, and IIS-1633363, as well as by the Academy of Finland project (CARMA), INFOTECH project (NOOR), and Kvantum Institute strategic project (SAFARI).

I. INTRODUCTION

Intelligent transportation systems (ITSs) will be a major component of tomorrow's smart cities. In essence, ITSs will provide a much safer and more coordinated traffic network by using efficient traffic management approaches [2]. One promising ITS service is the so-called *autonomous vehicular platoon system*, which is essentially a group of vehicles that operate together and continuously coordinate their speed and distance. By allowing autonomous vehicles to self-organize into a platoon, the road capacity can increase so as to prevent traffic jams [3]. Also, vehicles in the platoon can raise the fuel efficiency [4]. Furthermore, platoons can provide passengers with more comfortable trips, especially during long travels [5].

To reap the benefits of platooning, one must ensure that each vehicle in the platoon has enough awareness of its relative distance and velocity with its surrounding vehicles. This is needed to enable vehicles in a platoon to coordinate their acceleration and deceleration. In particular, enabling autonomous platooning requires two technologies: vehicle-to-vehicle (V2V) communications [6] and cooperative adaptive cruise control (CACC) [7]. V2V communications enable vehicles to exchange information, such as high definition (HD) maps, velocity, and acceleration [8]. Meanwhile, CACC is primarily a control system that allows control of the distances between vehicles using information collected by sensors and V2V links. Effectively integrating the operation of the CACC system and the V2V communication network is central for successful platooning in ITSs.

Nevertheless, due to dynamic on-vehicle data processing rate and the uncertainty of the wireless channel, the V2V communication links among vehicles will inevitably suffer from time-varying delays. Unfortunately, if the delayed information is used in the design of the autonomous vehicles' control system, such information can jeopardize the stable operation of the platoon [9]. Therefore, to maintain the stability of a platoon, the control system must be robust to such wireless transmission delays. To this end, one must jointly design the control and wireless systems of a platoon to guarantee low latency and stability.

The prior art on vehicular platooning can be grouped into two categories. The first category focuses on the performance analysis, such as interference management [10]–[13], coverage analysis [14], and transmission delay analysis [15]–[17], for the inter-vehicle communication network. The second category designs control strategies that guarantee the stability of the platoon system. Such strategies include adaptive cruise control (ACC) [18], enhanced ACC [19], and connected

cruise control (CCC) [20]. However, these works are limited in two aspects. The communication-centric works in [10]–[17] completely abstract the control system and do not study the impact of wireless communications on the platoon’s stability. Meanwhile, the control-centric works in [18]–[20] focus solely on the stability, while assuming a deterministic performance from the communication network. Such an assumption is not practical for platoons that coexist with 5G cellular networks, since interference from uncoordinated cochannel transmissions by other users, vehicles, and platoons can substantially impact the system’s performance. Clearly, despite the interdependent performance of communication and control systems in a platoon, there is a lack in existing works that jointly study the wireless and control system performance for vehicular platoons.

The main contribution of this paper is a novel, integrated control system and V2V wireless communication network framework for autonomous vehicular platoons. In particular, we first analyze the stability of the control system in a platoon, and, then, we determine the maximum tolerable transmission delay to maintain the stability of the platoon. Next, we use stochastic geometry and queuing theory to perform end-to-end delay analysis for the V2V communication link between two consecutive vehicles in the platoon. Based on the maximum wireless system delay and the theoretical end-to-end delay, we conduct reliability analysis for the wireless communication network. Here, reliability is defined as the possibility of the wireless system meeting the maximum delay requirements from the control system. Finally, we optimize the design of the control system to improve the reliability of the communication network. *To our best knowledge, this is the first work that considers the joint design of control and communication system performance for a wirelessly connected autonomous platoon.* The novelty of this work lies in the following key contributions:

- We propose an integrated control system and V2V wireless communication performance analysis framework to guarantee the overall operation of wirelessly connected vehicular platoons. In particular, we analyze two types of control system stability, plant stability and string stability, for the platoon, and derive the maximum wireless system delay that guarantees both types of stability. We then consider a highway model that models the distribution of platoon vehicles and non-platoon vehicles and derive the complementary cumulative density function (CCDF) for the signal-to-interference-plus-noise-ratio (SINR) of V2V communication links. Given the derived CCDF expression, we make use of queuing theory to determine the end-to-end wireless system delay, including queuing, processing,

and transmission delay for the V2V link in the platoon.

- We use the derived delay to study how the wireless network can meet the control system's delay needs. In particular, we derive a lower bound on the wireless network reliability (in terms of delay) needed to guarantee plant and string stability. In addition, we find an approximated reliability expression for vehicular network scenarios in which the wireless system delay is dominated by the transmission delay.
- We propose two optimization mechanisms to effectively design the control system as to improve the reliability of the wireless network. In particular, we find the optimal control system parameters that maximize the lower bound and the approximated values of the wireless network reliability.
- Simulation results corroborate the stability and SINR analysis and validate the effectiveness of the proposed joint control and communication framework. The results show how key parameters, such as the distribution density of non-platoon vehicles, packet size, spacing between two platoon vehicles, and platoon size, affect the reliability of a platoon. The results also show that, by optimizing the control system, the approximated reliability and the reliability lower bound of the wireless network can increase by as much as 25% and 30%, respectively.
- The proposed framework provides important guidelines to jointly design the wireless network and the control system for platoon systems. In particular, on the one hand, one should properly select the number of followers, the frequency bandwidth, and the spacing between two consecutive vehicles in the platoon system to ensure the stability of the control system. On the other hand, one can optimize the design of the control system, i.e., selecting proper control parameters, to alleviate the constraints on the wireless system delay and thereby improve the reliability of the wireless network.

The rest of the paper is organized as follows. Section II presents the system model. In Section III, we perform stability analysis for the autonomous platoon. The end-to-end delay and reliability analysis are presented in Section IV. Section V shows how to optimize the design of the control system. Section VI provides the simulation results, and conclusions are drawn in Section VII.

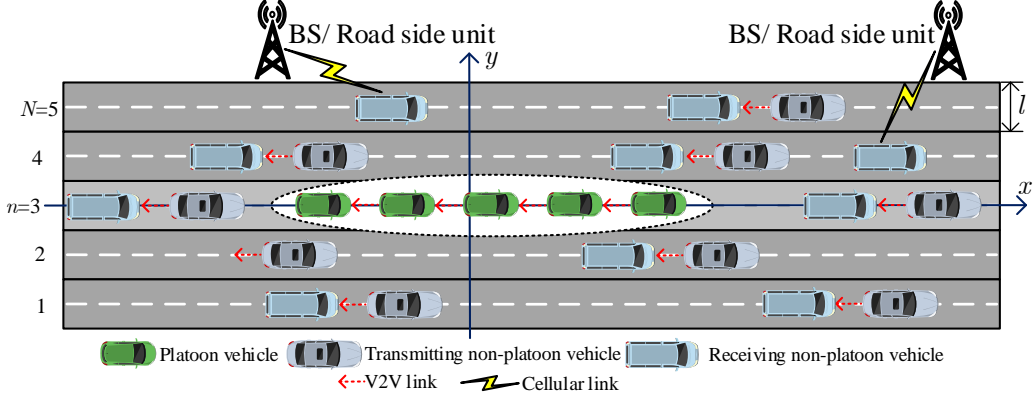


Fig. 1. A highway traffic model where vehicles in the dashed ellipse operate in a platoon and other vehicles out of the platoon drive individually.

II. SYSTEM MODEL

A. Highway Traffic Model

Consider a highway traffic model that is composed of a number of autonomous vehicles driving in a platoon and multiple vehicles driving individually, as shown in Fig. 1. All vehicles (inside and outside the platoon) communicate with one another using V2V communications. The vehicles can also transmit information to existing base stations (BSs) or road side units. Each lane in the highway model has the same width l , and vehicles are considered to travel along the horizontal axes in these lanes. As shown in Fig. 1, we label all N lanes based on their relative locations and we assume that platoon vehicles are moving in platoon lane n while the other $N - 1$ lanes are designated as non-platoon lanes. Accordingly, we define the set Φ of transmitting vehicles driving on non-platoon lanes and the set Ψ of transmitting non-platoon vehicles on the platoon lane. In particular, Φ consists of multiple subsets Φ_i , $i \leq N - 1$, of transmitting non-platoon vehicles on non-platoon lane i . However, set Ψ is only composed of two subsets of transmitting vehicles: one subset Ψ_1 of vehicles driving ahead of the platoon and another subset Ψ_2 behind the platoon.

To capture the distribution of transmitting non-platoon vehicles in the highway, we make use of spatial point processes from stochastic geometry. In particular, we characterize the distribution of transmitting vehicles on non-platoon lane $i \neq n$, as a homogeneous Poisson point process (PPP) with density λ_i . Moreover, for the platoon lane, the transmitting vehicles driving ahead of the platoon follow a nonhomogeneous PPP [21] where the distribution density for points ahead of the platoon is $\lambda_n^{(1)}$ and the density for points elsewhere is 0. Similarly, the transmitting vehicles driving behind the platoon also follow a nonhomogeneous PPP where the distribution density

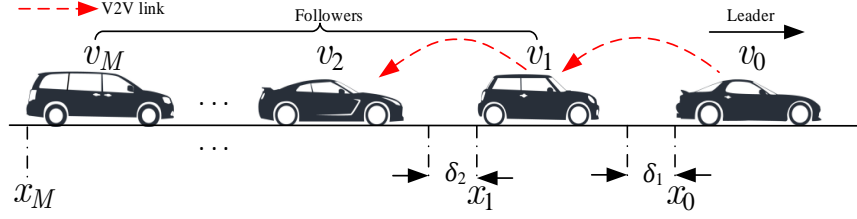


Fig. 2. Leader-follower model: a vehicular platoon with one leader and M followers.

of points behind the platoon is $\lambda_n^{(2)}$ and the density for points elsewhere is 0. Furthermore, as shown in Fig. 1, we consider a Cartesian coordinate system centered on the rear bumper of an arbitrarily selected platoon vehicle. In this case, the rear bumper location of each vehicle in the highway model can be mathematically represented using the coordinate system. For example, for a vehicle that is sharing the same lane with the platoon, the location can be expressed as $(x, 0)$, where x is the signed distance to the centered vehicle. However, for vehicle driving on lane different from the platoon lane, the corresponding location is $(x, (i - n)l)$, where x captures the signed distance to the y axis, and i denotes the lane number.

For vehicles inside the platoon, we consider a leader-follower model [7], as shown in Fig. 2. The leader-follower model is composed of a set \mathcal{M} of $M+1$ cars where the leading vehicle is the leader and the remaining M vehicles are the followers. The location of each vehicle in the platoon is captured by the rear bumper position $(x_i, 0)$. For each vehicle, an embedded radar can sense the distance between its rear bumper and the rear bumper of the preceding vehicle. Moreover, every vehicle can communicate with its neighbors via V2V links to exchange a variety of information such as critical information (e.g., velocity, acceleration, HD maps), and non-critical information (e.g., videos). Such information exchange can help the autonomous vehicle increase awareness of the environment and further coordinate its operation [8].

B. Channel Model and Interference Analysis

For V2V communications, we assume a V2V underlay network where the available cellular bandwidth ω is reused by all V2V links outside the platoon. Meanwhile, to facilitate simultaneous V2V communications and avoid interference among vehicles inside the platoon, we consider an orthogonal frequency-division multiple access (OFDMA) scheme, with the number of subcarriers being equal to the number of followers, i.e., subcarriers are allocated orthogonally and uniformly to V2V links in the platoon. However, due to bandwidth sharing with non-platoon vehicles, the followers will encounter interference from other V2V links outside the platoon. According to the work in [22], we model V2V channels in the platoon as independent Nakagami channels

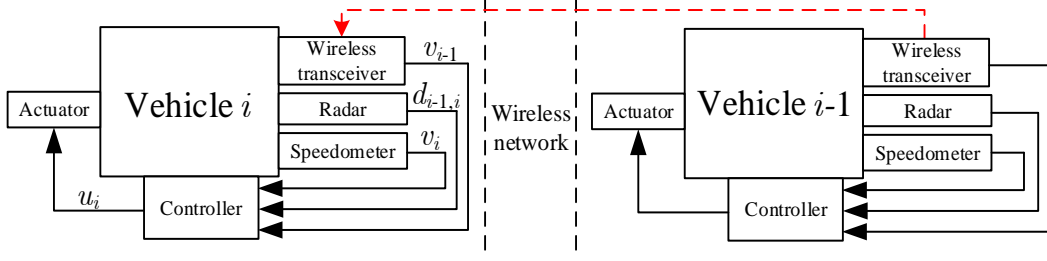


Fig. 3. Basic structure of a platoon system.

with parameter m . Therefore, in the platoon, the received power at any follower $i \in \mathcal{M}$ from the transmission of platoon car $i-1$ by using subcarrier j is $P_{i-1,i}^j(t) = P_t g_{i-1,i}^j(t) (d_{i-1,i}(t))^{-\alpha}$, where P_t is the transmit power of each vehicle, $g_{i-1,i}^j(t)$ is the Nakagami channel gain that follows a gamma distribution with shape parameter m , $d_{i-1,i}(t)$ is the distance between vehicles $i-1$ and i inside the platoon, and α is the path loss exponent. We model the channels from non-platoon vehicles to an arbitrary platoon vehicle i as independent Rayleigh fading channels [23]. With this in mind, the overall interference at car i is the sum of two following interference terms:

$$I_i^{\text{non-platoon}}(t) = \sum_{j_1=1}^{n-1} \sum_{c \in \Phi_{j_1}} P_t g_{c,i}(t) (d_{c,i}(t))^{-\alpha} + \sum_{j_2=n+1}^N \sum_{c \in \Phi_{j_2}} P_t g_{c,i}(t) (d_{c,i}(t))^{-\alpha}, \quad (1)$$

$$I_i^{\text{platoon}}(t) = \sum_{j_3=1}^2 \sum_{c \in \Psi_{j_3}} P_t g_{c,i}(t) (d_{c,i}(t))^{-\alpha}, \quad (2)$$

where $d_{c,i}(t)$ denotes the distance between vehicles c and i , and $g_{c,i}(t)$ refers to the channel gain from vehicle c to i at time t , which follows an exponential distribution with mean equal to 1. Using (1) and (2), the SINR of the V2V link on subcarrier j from car $i-1$ to i will be:

$$\gamma_{i-1,i}^j(t) = \frac{P_{i-1,i}^j(t)}{I_i^{\text{non-platoon}}(t) + I_i^{\text{platoon}}(t) + \sigma^2}, \quad (3)$$

where σ^2 is the variance of Gaussian noise. Using (3), we can obtain the throughput of the V2V link between vehicles $i-1$ and i as $R_{i-1,i}^j(t) = \frac{\omega}{M} \log_2(1 + \gamma_{i-1,i}^j(t))$.

C. Control Model

To realize the target spacing for the platoon, the CACC system in each vehicle will brake or accelerate according to the difference between the actual distance and target spacing slot to the preceding vehicle. That is, if the difference is positive, the vehicle must speed up so that the distance to the preceding car meets the platoon's target spacing. Otherwise, the vehicle must slow down. This distance difference is defined as the spacing error $\delta_i(t)$:

$$\delta_i(t) = x_{i-1}(t) - x_i(t) - L_t, i \in \mathcal{M}, \quad (4)$$

where L_t is the target spacing for the platoon system. The distance difference, $d_{i-1,i}(t) = x_{i-1}(t) - x_i(t)$, is commonly known as the *headway*, which can be measured instantly by the vehicle's built-in radar sensor, as shown in Fig. 3. In addition, the velocity error will be:

$$z_i(t) = v_i(t) - v_t, \quad (5)$$

where $v_i(t)$ represents the velocity of vehicle i at time t , and v_t is the target velocity for the platoon system. Similar to the optimal velocity model (OVM) introduced in [24], to realize the stability of a platoon system, the acceleration or deceleration of each vehicle must be determined by two components: 1) the difference between headway-dependent and actual velocities, and 2) the velocity difference between a given vehicle and its preceding vehicle. Hence, we can use the following control law to determine the acceleration $u_i(t)$ of vehicle i [24]:

$$u_i(t) = a_i(t)[V(d_{i-1,i}(t)) - v_i(t)] + b_i(t)[v_{i-1}(t - \tau_{i-1,i}(t)) - v_i(t)], \quad (6)$$

where $\tau_{i-1,i}(t)$ captures the wireless system delay between vehicle i and its preceding vehicle, $a_i(t)$ is the associated gain of vehicle i for the difference of the headway-dependent velocity and the actual speed, and $b_i(t)$ is the associated gain of vehicle i for the velocity difference between cars $i - 1$ and i . Note that the associated gains $a_i(t)$ and $b_i(t)$ essentially capture the sensibility of the CACC system to respond to changes of the distance and velocity. The headway-dependent velocity $V(d)$ should satisfy following properties: 1) in dense traffic, the vehicle will stop, i.e., $V(d) = 0$ for $d \leq d_{\text{dense}}$, 2) in sparse traffic, the vehicle can travel with its maximum speed $V(d) = v_{\text{max}}$, which is also called free-flow speed, for $d \geq d_{\text{sparse}}$, and 3) when $d_{\text{dense}} < d < d_{\text{sparse}}$, $V(d)$ is a monotonically increasing function of d . We define the function $V(d)$ similar to [25]:

$$V(d) = \begin{cases} 0, & \text{if } d < d_{\text{dense}}, \\ v_{\text{max}} \times \left(\frac{d - d_{\text{dense}}}{d_{\text{sparse}} - d_{\text{dense}}} \right), & \text{if } d_{\text{dense}} \leq d \leq d_{\text{sparse}}, \\ v_{\text{max}}, & \text{if } d_{\text{sparse}} < d. \end{cases} \quad (7)$$

To guarantee the stable operation of the platoon system, it is essential to jointly consider the design of the communication and control systems. In particular, on the one hand, for a given control system setup, one can design the wireless network so as to meet the delay requirement of V2V links and prevent the instability of the control system. On the other hand, given the state of the wireless system, one can also optimize the design of the control system to relax the delay requirements for the communication system. In the following sections, we will first conduct stability analysis for the control system and find the wireless system delay requirements

to realize the stable operation of the control system. Then, based on the distribution of vehicles, we derive the CCDF of the SINR of V2V links in the platoon. To model the delay, we consider two queues in tandem for the V2V link, and leverage queuing theory to derive the end-to-end delay, including queuing, processing, and transmission delay. Then, we derive the lower bound and approximated expressions for the wireless system reliability, defined as the probability that the wireless system meets the delay requirements from the control system. Moreover, we study the optimal design for the control system to maximize the derived reliability metrics of the wireless network.

III. STABILITY ANALYSIS OF THE CONTROL SYSTEM

For the leader-follower platoon model, the inevitable wireless system delay in (6) can negatively impact the stability of the platoon system. Here, we perform stability analysis for the control system in presence of a wireless system delay. We analyze two types of stability: plant stability and string stability [7]. Plant stability focuses on the convergence of error terms related to the inter-vehicle distance and velocity, while string stability pertains to the error propagation across the platoon. Using this stability analysis, we obtain the wireless system delay thresholds that can ensure plant and string stability for the control system.

A. Plant Stability

Plant stability requires all followers in a platoon to drive with the same speed as the leader and maintain a target distance from the preceding vehicle. In other words, plant stability requires both the spacing and speed errors of each vehicle to converge to zero. To prove the convergence, we first take the first-order derivative of (4) and (5) as:

$$\begin{cases} \dot{\delta}_i(t) = z_{i-1}(t) - z_i(t), \\ \dot{z}_i(t) = A_i \delta_i(t) + B_i z_{i-1}(t - \tau_{i-1,i}(t)) - C_i z_i(t), \end{cases} \quad (8)$$

where $\dot{\delta}_i(t)$ and $\dot{z}_i(t)$ are variables differentiated with respect to time t , $A_i = \frac{a_i(t)v_{\max}}{d_{\text{sparse}} - d_{\text{dense}}}$, $B_i = b_i(t)$, and $C_i = a_i(t) + b_i(t)$. Since the leading vehicle with index 0 always drives with the target velocity and has no car ahead of it, its velocity (spacing) error is $z_0(t) = 0$ ($\delta_0(t) = 0$). Also, as the channel gains of different V2V links follow the same distribution and two adjacent vehicles in a platoon are always close to each other, we assume that the time delay $\tau_{i-1,i}(t) = \tau(t)$, $\forall i \in \mathcal{M}$.

Then, after the BS collects spacing and velocity errors for all of the followers, we can find the augmented error state vector $e(t)=[\delta_1(t), \delta_2(t), \dots, \delta_M(t), z_1(t), z_2(t), \dots, z_M(t)]^T$ and obtain

$$\dot{e}(t) = \begin{bmatrix} \mathbf{0}_{M \times M} & \mathbf{\Omega}_1 \\ \mathbf{\Omega}_2 & \mathbf{\Omega}_3 \end{bmatrix} e(t) + \begin{bmatrix} \mathbf{0}_{M \times M} & \mathbf{0}_{M \times M} \\ \mathbf{0}_{M \times M} & \mathbf{\Omega}_4 \end{bmatrix} e(t - \tau(t)), \quad (9)$$

where

$$\mathbf{\Omega}_1 = \begin{bmatrix} -1 & 0 & 0 & \dots & 0 & 0 \\ 1 & -1 & 0 & \dots & 0 & 0 \\ 0 & 1 & -1 & \dots & 0 & 0 \\ \vdots & \vdots & \vdots & \ddots & \vdots & \vdots \\ 0 & 0 & 0 & \dots & 1 & -1 \end{bmatrix}_{M \times M}, \quad (10)$$

$$\mathbf{\Omega}_2 = \text{diag}\{A_1, A_2, \dots, A_M\}_{M \times M}, \mathbf{\Omega}_3 = \text{diag}\{-C_1, -C_2, \dots, -C_M\}_{M \times M}, \quad (11)$$

$$\mathbf{\Omega}_4 = \begin{bmatrix} 0 & 0 & 0 & \dots & 0 & 0 \\ B_2 & 0 & 0 & \dots & 0 & 0 \\ 0 & B_3 & 0 & \dots & 0 & 0 \\ \vdots & \vdots & \vdots & \ddots & \vdots & \vdots \\ 0 & 0 & 0 & \dots & B_M & 0 \end{bmatrix}_{M \times M}, \quad (12)$$

and $e(t-\tau(t)) = [\delta_1(t-\tau(t)), \delta_2(t-\tau(t)), \dots, \delta_M(t-\tau(t)), z_1(t-\tau(t)), z_2(t-\tau(t)), \dots, z_M(t-\tau(t))]^T$.

For ease of presentation, we rewrite $\mathbf{M}_1 = \begin{bmatrix} \mathbf{0}_{M \times M} & \mathbf{\Omega}_1 \\ \mathbf{\Omega}_2 & \mathbf{\Omega}_3 \end{bmatrix}$, $\mathbf{M}_2 = \begin{bmatrix} \mathbf{0}_{M \times M} & \mathbf{0}_{M \times M} \\ \mathbf{0}_{M \times M} & \mathbf{\Omega}_4 \end{bmatrix}$, and replace $e(t)$ with e hereinafter. Since plant stability requires the spacing and velocity errors to approach zero, the error vector $e(t) = \mathbf{0}_{2M \times 2M}$ should be asymptotically stable.

To guarantee the plant stability for a platoon, the delay experienced by a V2V link should be below a threshold. Next, we derive the delay threshold to guarantee plant stability.

Theorem 1. *The plant stability of the system in (6) can be guaranteed if the maximum delay of the V2V link in the platoon satisfies:*

$$\tau \leq \tau_1 = \frac{\lambda_{\min}(-\mathbf{M}_1 - \mathbf{M}_2 - (\mathbf{M}_1 + \mathbf{M}_2)^T)}{\lambda_{\max}(\mathbf{M}_2 \mathbf{M}_1 \mathbf{M}_1^T \mathbf{M}_2^T + \mathbf{M}_2 \mathbf{M}_2 \mathbf{M}_2^T \mathbf{M}_2^T + 2k \mathbf{I}_{2M \times 2M})}, \quad (13)$$

where $\lambda_{\max}(\cdot)$ and $\lambda_{\min}(\cdot)$ represent the maximum and minimum eigenvalues of the corresponding matrix, respectively.

Proof: Please refer to Appendix A. ■

Hence, when $\tau \leq \tau_1$, following vehicles will eventually drive with the same speed as the leading vehicle and keep an identical distance to the corresponding preceding vehicles.

B. String Stability

Beyond plant stability, we must ensure that the platoon is *string stable*. In particular, if the disturbances, in terms of velocity or distance, of preceding vehicles do not amplify along with the platoon, the system can have string stability and the safety of the system can be secured [3]. To analyze string stability, we also consider the wireless delay $\tau_{i-1,i}(t) = \tau(t), \forall i \in \mathcal{M}$, between vehicles $i-1$ and i . Hence, after conducting the Laplace transform on the two equations in (8), we can obtain the transfer function between two adjacent vehicles as follows:

$$T(s) = \frac{z_i(s)}{z_{i-1}(s)} = \frac{A + sBe^{-s\tau(t)}}{s^2 + Cs + A}. \quad (14)$$

By using the Padé approximation, $e^x \approx \frac{1+0.5x}{1-0.5x}$ [26], we further simplify (14) and derive the maximum wireless system delay needed to maintain the string stability for the platoon system.

Theorem 2. *The string stability of the system in (6) can be guaranteed if the maximum delay of the V2V link in the platoon satisfies:*

$$\tau \leq \tau_2 = \frac{C^2 - 2A - B^2}{2AB}. \quad (15)$$

Proof: Please refer to Appendix B. ■

Thus, if $\tau \leq \tau_2$, the spacing error and velocity error will not amplify along the string of vehicles, guaranteeing the platoon's safety. To guarantee both plant and string stability for a platoon, we must ensure that the delay encountered by the V2V link is such that $\tau \leq \min(\tau_1, \tau_2)$.

IV. END-TO-END LATENCY ANALYSIS OF THE WIRELESS NETWORK

From the results presented in Section III, to realize the stability for the control system, the wireless V2V network must guarantee that the maximum delay between two consecutive vehicles in the platoon is less than a threshold. To quantify such wireless system delay, we need to know how a data packet propagates among vehicles as well as the key factors that affect the delay inside the platoon. As shown in Fig. 4(a), vehicular network information, such as velocity and acceleration, will be first collected by various sensing units in the vehicle. Here, sensing units consist of analog-to-digital converters (ADCs), which convert analog data from the sensor to digital data that can be processed by the processor. Then, the vehicle will process the data and

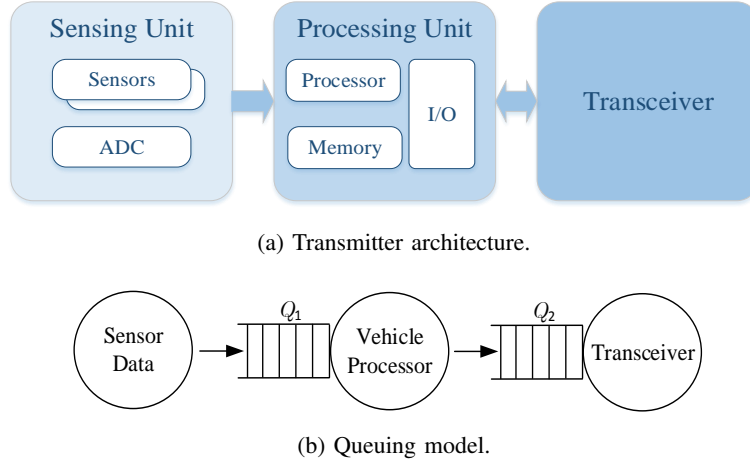


Fig. 4. Data path inside a transmitting vehicle.

convert it into analog data, which will be finally transmitted by transceiver to other vehicles via V2V links. Such information exchange is needed because vehicles can have more awareness of the nearby environment so as to know where to go and when to stop [27]. This process will occur periodically because the environment both inside and outside of the platoon system is changing all the time. To capture the V2V communication delay, we define the queuing model shown in Fig. 4(b) with no time delay accounted for sensor information collection and ADCs processes. In particular, after being converted at ADCs, each information packet experiences queuing delay and the processing delay at the processor (the first queue Q_1), and, then, the packet will encounter the queuing delay and the transmission delay at the transceiver (the second queue Q_2). We define the total time delay from the transmitting vehicle to the receiving vehicle of a V2V link in the platoon as the *end-to-end delay*, including the time spent in queues Q_1 and Q_2 .

A. Queuing Delay and Processing Delay in Queue Q_1

Once a vehicle collects the data using its sensors, data needs to be processed locally and then sent to the transceiver. To model the delay at the processor, similar to [28], we consider a Poisson arrival process of the sensor packets with rate λ_a and a buffer with infinite size for the processor. Also, we consider that the processor serves the incoming data based on a first come, first serve policy. Moreover, the service time of the vehicle processor follows an exponential distribution with rate parameter $\mu_1 > \lambda_a$ for guaranteeing the stability of the first queue [29]. Similar to the dynamic voltage scaling technique introduced in [30], the voltage for the processor will dynamically change and the processing rate will change accordingly. We assume that the rate parameter μ_1 can be expressed as a monotonically decreasing function of the distance to the

preceding vehicle. Consequently, when the distance between two vehicles is small, the service rate μ_1 will increase so that the processing time and the queuing delay in queue Q_1 can be reduced. To guarantee the decreasing monotonicity of μ_1 , we propose the following policy for μ_1 :

$$\mu_1(d) = \begin{cases} \lambda_a, & \text{if } d_{\max}^{\text{radar}} < d, \\ \frac{\lambda_a - \mu_{\max}}{d_{\max}^{\text{radar}}}d + \mu_{\max}, & \text{otherwise,} \end{cases} \quad (16)$$

where d_{\max}^{radar} is the maximum distance detected by the embedded radar sensor, and μ_{\max} is the maximum rate of the vehicle's processor. We assume that each vehicle has only one processor, so the first queue can be modeled as an M/M/1 queue. Thus, according to [29], the average queuing delay of a packet at the vehicle's processor can be expressed as $\bar{T}_1^q = \frac{\lambda_a}{\mu_1(d)(\mu_1(d) - \lambda_a)}$. The mean processing time of each packet at the processor can be captured by $\bar{T}_1^s = 1/\mu_1(d)$. Based on \bar{T}_1^q and \bar{T}_1^s , we can obtain the average delay for each packet at the first queue Q_1 :

$$\bar{T}_1 = \bar{T}_1^q + \bar{T}_1^s = \frac{\lambda_a}{\mu_1(d)(\mu_1(d) - \lambda_a)} + \frac{1}{\mu_1(d)}. \quad (17)$$

B. Queuing Delay and Transmission Delay in Queue Q_2

In queue Q_2 , the processing rate of the transceiver is determined by the channel quality and, whenever the buffer is not empty, any incoming packet will have to wait in the buffer. According to the Burke's theorem [31], when the service rate is bigger than the arrival rate for an M/M/1 queue, the departure process can be modeled as a Poisson process with the same rate. In this case, given that $\mu_1 > \lambda_a$ is always satisfied in the first queue Q_1 , the incoming packet for the second queue Q_2 follows a Poisson process with rate λ_a . In addition, we assume an infinite buffer size and a first come, first serve policy for Q_2 . Furthermore, the service rate in the second queue Q_2 is essentially the V2V data rate which will follow a general distribution because of the uncertainty of the wireless channel. To characterize such channel uncertainty, we make use of stochastic geometry to analyze the V2V communication performance. In particular, we assume that the rear bumper of platoon vehicle i is located at the origin of the Cartesian system. As explained in Section II, vehicle i will experience interference from transmitting non-platoon vehicles on any lane. Next, we take vehicle i as an example and use the Laplace transforms of the experienced interference generated by non-platoon vehicles in the following lemmas.

Lemma 1. For an arbitrary vehicle i in the platoon, the Laplace transform of the interference $I_i^{\text{non-platoon}}(t)$ from transmitting vehicles on the non-platoon lanes in (1) can be given by:

$$\begin{aligned} \mathcal{L}_i^{\text{non-platoon}}(s) = & \prod_{j_1=1}^{n-1} \exp \left[-\lambda_{j_1} \int_{(n-j_1)l}^{\infty} \left(1 - \frac{1}{1 + sP_t r^{-\alpha}} \right) \frac{2r}{\sqrt{r^2 - (n-j_1)^2 l^2}} dr \right] \\ & \times \prod_{j_2=n+1}^N \exp \left[-\lambda_{j_2} \int_{(j_2-n)l}^{\infty} \left(1 - \frac{1}{1 + sP_t r^{-\alpha}} \right) \frac{2r}{\sqrt{r^2 - (j_2-n)^2 l^2}} dr \right]. \end{aligned} \quad (18)$$

Proof: Please refer to Appendix C. ■

Lemma 2. For an arbitrary vehicle i in the platoon, the Laplace transform of the interference $I_i^{\text{platoon}}(t)$ from transmitting non-platoon vehicles on the platoon lane in (2) can be given by:

$$\mathcal{L}_i^{\text{platoon}}(s) = \exp \left[-\lambda_n^{(1)} \int_{d_i^{\text{head}}}^{\infty} \left(1 - \frac{1}{1 + sP_t r^{-\alpha}} \right) dr - \lambda_n^{(2)} \int_{d_i^{\text{tail}}}^{\infty} \left(1 - \frac{1}{1 + sP_t r^{-\alpha}} \right) dr \right], \quad (19)$$

where $d_i^{\text{head}} = x_0 - x_i$ and $d_i^{\text{tail}} = x_i - x_M$ are the distance from vehicle i to the head and the tail of the platoon, respectively.

Proof: The proof is similar to Appendix C. However, for vehicles driving on the platoon lane, the distance is directly equal to the horizontal distance. ■

Based on the Laplace transforms of interference terms in (18) and (19), we can obtain the expressions of the mean and variance of the service time D for a single packet as follow.

Theorem 3. For a single packet transmitted from vehicle $i-1$ to vehicle i in the platoon, the mean and variance of the service time D can be expressed as

$$\mathbb{E}(D) = \int_0^{\infty} \frac{SM}{\omega \log_2(1 + \theta)} f(\theta) d\theta, \quad (20)$$

$$\text{Var}(D) = \int_0^{\infty} \frac{S^2 M^2}{\omega^2 (\log_2(1 + \theta))^2} f(\theta) d\theta - \left(\int_0^{\infty} \frac{SM}{\omega \log_2(1 + \theta)} f(\theta) d\theta \right)^2, \quad (21)$$

where S is the packet size in bits, and $f(\theta) = -\frac{d\mathbb{F}(\theta)}{d\theta}$ with

$$\begin{aligned} \mathbb{F}(\theta) = \mathbb{P}(\gamma_{i-1,i} > \theta) = & \sum_{k=1}^m (-1)^{k+1} \binom{m}{k} \exp \left(\frac{-k\eta\theta d_{i-1,i}^{\alpha}}{P_t} \sigma^2 \right) \mathcal{L}_i^{\text{non-platoon}} \left(\frac{k\eta\theta d_{i-1,i}^{\alpha}}{P_t} \right) \\ & \mathcal{L}_i^{\text{platoon}} \left(\frac{k\eta\theta d_{i-1,i}^{\alpha}}{P_t} \right), \end{aligned} \quad (22)$$

and $\eta = m(m!)^{-\frac{1}{m}}$.

Proof: Please refer to Appendix D. ■

Given the distribution of incoming packets and the infinite storage capacity, the second queue can be modeled as an M/G/1 queue. Thus, according to the well-known Pollaczek-Khinchine formula [32], we can determine the average delay, including the transmission delay and the waiting time, in the second queue Q_2 as:

$$\bar{T}_2 = \frac{\rho_2 + \lambda_a \mu_2 \text{Var}(D)}{2(\mu_2 - \lambda_a)} + \mu_2^{-1}, \quad (23)$$

where $\mu_2 = 1/\mathbb{E}(D)$ and $\rho_2 = \lambda_a \mathbb{E}(D)$. We assume that the receiving vehicle can be aware of the velocity of the preceding vehicle once it receives the information packet over wireless communications. Thus, the average end-to-end delay can be expressed as $\bar{T} = \bar{T}_1 + \bar{T}_2$.

C. Control-Aware Reliability of the Wireless Network

To assess the performance of the integrated control and communication system, we introduce a notion of reliability for the wireless network, defined as the probability of the instantaneous delay in the wireless network meeting the control systems delay needs. This reliability measure allows for the characterization of the performance of the wireless network that can guarantee the stability of the platoon's control system. Moreover, we will use this deviation to gain insights on the design of wireless networks that can sustain the operation of vehicular platoons. These insights include characterizing how much transmission power and bandwidth are needed to realize a target reliability. However, it is challenging to directly derive the probability density functions (PDFs) of the instantaneous wireless network delay. The reason is that, in queuing theory, the average waiting time is not derived based on the PDF of the instantaneous waiting time. Instead, the average waiting time is calculated by first deriving the average number of packets staying in the queue and then using Little's law, which is the relationship among the number of packets, the incoming packet rate, and the waiting time [29]. As the end-to-end delay is composed of queuing delay, processing delay, and transmission delay, finding the exact PDFs for the instantaneous wireless system delay and the reliability is thereby challenging. Alternatively, we will derive a lower bound for the reliability of the wireless network in the following theorem.

Theorem 4. *For the followers in a platoon system, when the average wireless system delay \bar{T} is smaller than the requirement $\min(\tau_1, \tau_2)$ of the stability of the control system, a lower bound*

for the reliability of the wireless network can be given by:

$$\mathbb{P}(T_1+T_2 \leq \min(\tau_1, \tau_2)) \geq \max \left(1 - \frac{\bar{T}_1 + \bar{T}_2}{\min(\tau_1, \tau_2)}, 1 - \exp \left(-\frac{\bar{T}_1 + \bar{T}_2 - \min(\tau_1, \tau_2) \ln \left(\frac{\min(\tau_1, \tau_2)}{\bar{T}_1 + \bar{T}_2} \right)}{\min(\tau_1, \tau_2)} \right) \right), \quad (24)$$

where τ_1 and τ_2 are the delay requirements to guarantee plant and string stability, respectively, for the control system.

Proof: Please refer to Appendix E. ■

Corollary 1. *By substituting the delay requirement $\min(\tau_1, \tau_2)$ by τ_1 or τ_2 in (24), the lower bounds of the reliability for the wireless network guaranteeing either plant stability or string stability can be obtained.*

Given the lower bounds in Theorem 4 and Corollary 1, we can deduce key guidelines for the joint design of the wireless network and the control system. For instance, to guarantee that the reliability exceeds a threshold, e.g., 95%, we can ensure that the lower bound in (24) is equal to the threshold by choosing proper values for the wireless network parameters, such as bandwidth and transmission power. Meanwhile, we can increase $\min(\tau_1, \tau_2)$ by properly selecting the control parameters a_i and $b_i, i \in \mathcal{M}$, for the control system to guarantee that the lower bound is equal to the threshold as well. Moreover, next, we can obtain an approximated reliability expression if the wireless delay is dominated by the transmission delay.

Corollary 2. *When the vehicle's processor is highly capable and the incoming packet rate is small, the delay at Q_1 and the queuing delay at Q_2 are relatively small compared to the transmission delay at Q_2 . In this case, the wireless system delay is dominated by the transmission delay at Q_2 , and the reliability of the wireless network can be thereby approximated by:*

$$\mathbb{P}(T_1+T_2 \leq \min(\tau_1, \tau_2)) \approx \sum_{k=1}^m (-1)^{k+1} \binom{m}{k} \exp \left(\frac{-k\eta \left(2^{\frac{SM}{\omega \min(\tau_1, \tau_2)}} - 1 \right) d_{i-1,i}^\alpha}{P_t} \sigma^2 \right) \mathcal{L}_i^{\text{non-platoon}} \left(\frac{k\eta \left(2^{\frac{SM}{\omega \min(\tau_1, \tau_2)}} - 1 \right) d_{i-1,i}^\alpha}{P_t} \right) \mathcal{L}_i^{\text{platoon}} \left(\frac{k\eta \left(2^{\frac{SM}{\omega \min(\tau_1, \tau_2)}} - 1 \right) d_{i-1,i}^\alpha}{P_t} \right). \quad (25)$$

Proof: The proof is analogous to Appendix D and the difference is replacing θ with $2^{\frac{SM}{\omega \min(\tau_1, \tau_2)}} - 1$ in the CCDF (22) of SINR. ■

From Corollary 2, we can not only infer guidelines for the design of the wireless network and the control system to guarantee a promising reliability, but we can also observe how the interference and noise directly impact the ability of the wireless network to secure the stability of the control system. To mitigate such impacts, one needs to develop interference management and noise mitigation mechanisms. However, when the state of the wireless network is given, we can still guarantee a satisfactory reliability for the platoon system by optimizing the design of the control system, as explained next.

V. OPTIMAL CONTROLLER DESIGN

For a system with fixed control parameters, a_i and b_i , $i \in \mathcal{M}$, in the control law (6), we can meet the delay requirements in Theorems 1 and 2 by improving the wireless network performance. However, when the control parameters are not fixed, we can optimize the design of the control system to relax the constraints on the wireless network without jeopardizing the system stability. In particular, to improve the reliability of the wireless network, the optimization of the control system can be done depending on the capabilities of the processor and the arrival rate. For instance, for scenarios in which the processor is highly capable and the arrival rate is small, we can find control parameters for maximizing $\min(\tau_1, \tau_2)$ so as to improve the approximated reliability as per Corollary 2. In contrast, if we consider a general scenario, then we can directly maximize the lower bound as per Theorem 4.

A. Optimization of the Approximated Reliability

To improve the reliability of the wireless network in Corollary 2, we design the control system to maximize the smaller value between the two stability delay requirements, i.e., $\max \min(\tau_1, \tau_2)$. Here, we assume that the control parameters are the same for each vehicle at time t , i.e., $a_i(t) = a$ and $b_i(t) = b$, $i \in \mathcal{M}$, and the optimization problem can be formulated into the following form:

$$\max_{a,b} \tau \tag{26}$$

$$\text{s.t. } \tau \leq \min(\tau_1, \tau_2), \tag{27}$$

$$a_{\min} \leq a \leq a_{\max}, b_{\min} \leq b \leq b_{\max}, \tag{28}$$

where constraint (27) guarantees plant stability and string stability for the platoon system, and constraint (28) guarantees that both control parameters are selected within reasonable ranges.

Theorem 5. *The optimal control parameters that are the solutions to the optimization problem in (26)–(28) are given by:*

- $(a_{\text{opt}}, b_{\text{opt}})$ when $\frac{\partial \min(\tau_1, \tau_2)}{\partial a_{\text{opt}}} = 0$ and $\frac{\partial \min(\tau_1, \tau_2)}{\partial b_{\text{opt}}} = 0$,
- $(a_{\min}, b_{\text{opt}})$ when $\frac{\partial \min(\tau_1, \tau_2)}{\partial b_{\text{opt}}} = 0$ and $\frac{\partial \min(\tau_1, \tau_2)}{\partial a} \leq 0$ for $a_{\min} \leq a \leq a_{\max}$,
- $(a_{\max}, b_{\text{opt}})$ when $\frac{\partial \min(\tau_1, \tau_2)}{\partial b_{\text{opt}}} = 0$ and $\frac{\partial \min(\tau_1, \tau_2)}{\partial a} \geq 0$ for $a_{\min} \leq a \leq a_{\max}$,
- $(a_{\text{opt}}, b_{\min})$ when $\frac{\partial \min(\tau_1, \tau_2)}{\partial a_{\text{opt}}} = 0$ and $\frac{\partial \min(\tau_1, \tau_2)}{\partial b} \leq 0$ for $b_{\min} \leq b \leq b_{\max}$,
- $(a_{\text{opt}}, b_{\max})$ when $\frac{\partial \min(\tau_1, \tau_2)}{\partial a_{\text{opt}}} = 0$ and $\frac{\partial \min(\tau_1, \tau_2)}{\partial b} \geq 0$ for $b_{\min} \leq b \leq b_{\max}$,
- (a_{\min}, b_{\min}) when $\frac{\partial \min(\tau_1, \tau_2)}{\partial a} \leq 0$ and $\frac{\partial \min(\tau_1, \tau_2)}{\partial b} \leq 0$ for $a_{\min} \leq a \leq a_{\max}$ and $b_{\min} \leq b \leq b_{\max}$,
- (a_{\min}, b_{\max}) when $\frac{\partial \min(\tau_1, \tau_2)}{\partial a} \leq 0$ and $\frac{\partial \min(\tau_1, \tau_2)}{\partial b} \geq 0$ for $a_{\min} \leq a \leq a_{\max}$ and $b_{\min} \leq b \leq b_{\max}$,
- (a_{\max}, b_{\min}) when $\frac{\partial \min(\tau_1, \tau_2)}{\partial a} \geq 0$ and $\frac{\partial \min(\tau_1, \tau_2)}{\partial b} \leq 0$ for $a_{\min} \leq a \leq a_{\max}$ and $b_{\min} \leq b \leq b_{\max}$,
- (a_{\max}, b_{\max}) when $\frac{\partial \min(\tau_1, \tau_2)}{\partial a} \geq 0$ and $\frac{\partial \min(\tau_1, \tau_2)}{\partial b} \geq 0$ for $a_{\min} \leq a \leq a_{\max}$ and $b_{\min} \leq b \leq b_{\max}$.

Proof: Please refer to Appendix F. ■

Note that matrices in the numerator and denominator of (13) are symmetric, and, hence, we can use the inverse iteration algorithm and power iteration algorithm, introduced in [33], to approximately find the minimum eigenvalue for the matrix in the numerator and the maximum eigenvalue for the matrix in the denominator. Furthermore, we can identify whether $\frac{\partial \min(\tau_1, \tau_2)}{\partial a}$ and $\frac{\partial \min(\tau_1, \tau_2)}{\partial b}$ are positive or negative based on the range of a and b and, then, determine the optimal control parameters in Theorem 5.

B. Optimization of the Lower Bound for the Reliability

To increase the wireless network's reliability derived in Theorem 4, we can directly maximize the lower bound obtained in (24) by choosing proper a and b . In particular, the optimization function can be formulated as

$$\max_{a, b} \max \left(1 - \frac{\bar{T}_1 + \bar{T}_2}{\min(\tau_1, \tau_2)}, 1 - \exp \left(\bar{T}_1 + \bar{T}_2 - \min(\tau_1, \tau_2) \ln \left(\frac{\min(\tau_1, \tau_2)}{\bar{T}_1 + \bar{T}_2} \right) \right) \right), \quad (29)$$

$$\text{s.t. } \bar{T}_1 + \bar{T}_2 \leq \min(\tau_1, \tau_2), \quad (30)$$

$$a_{\min} \leq a \leq a_{\max}, b_{\min} \leq b \leq b_{\max}, \quad (31)$$

where constraint (30) is a necessary condition for calculating the lower bound of the reliability, and constraint (31) guarantees that both control parameters are selected in reasonable ranges.

Table. I. Simulation parameters.

Parameter	Description	Value
l	Width of each lane	3.7 m
N, n	Number of lanes and label of platoon lane	4, 4
P_t	Transmission power	27 dBm
m	Nakagami parameter	3 [22]
α	Path loss exponent	3
ω	Total bandwidth	40 MHz
σ^2	Noise variance	-174 dBm/Hz
v_{\max}	Maximum speed	30 m/s [7]
S	Packet size	3200 bits ¹ , 10000 bits
M	Number of followers	6
$d_{\text{sparse}}, d_{\text{dense}}$	Distance for sparse and dense traffic	35 m [7], 5 m [7]
λ_a, μ_{\max}	Incoming rate of packets and maximum processing rate for the processor	10 packets/s [34], 12000 packets/s [35]
d_{\max}^{radar}	Maximum distance detected by the radar sensor	200 m [36]

Theorem 6. *The optimal control parameters that are the solution to the optimization problem in (29)–(31) will be equal to the solutions derived in Theorem 5 as long as such control parameters can guarantee $\bar{T}_1 + \bar{T}_2 \leq \min(\tau_1, \tau_2)$.*

Proof: Please refer to Appendix G. ■

Using the two foregoing optimization problems, we can find appropriate parameters for the control mechanism to improve the performance of wireless networks. However, we note that changing the control system parameters may lead to an increase of the manufacturer cost and maintenance spending. Nevertheless, Theorems 5 and 6 still provide us with key guidelines on how to modify the control parameters to optimize the platoon's overall operation.

VI. SIMULATION RESULTS AND ANALYSIS

In this section, we will first validate the theoretical results in Sections III and IV by numerical results. Moreover, we present performance analysis for the integrated communication and control system based on the results in Sections IV and V. In particular, we consider a 10 kilometer-long highway segment with 4 lanes, and the lane with label $n = 4$ is the platoon lane. According to the empirical data collected by the Berkeley Highway Laboratory [38] and its analytical results [39], the density of vehicles on the highway is mostly in the range from 0.01 vehicle/m to

¹The packet size of 3200 bits is chosen based on the specifications for the Dedicated Short Range Communications (DSRC) safety messages length [37].

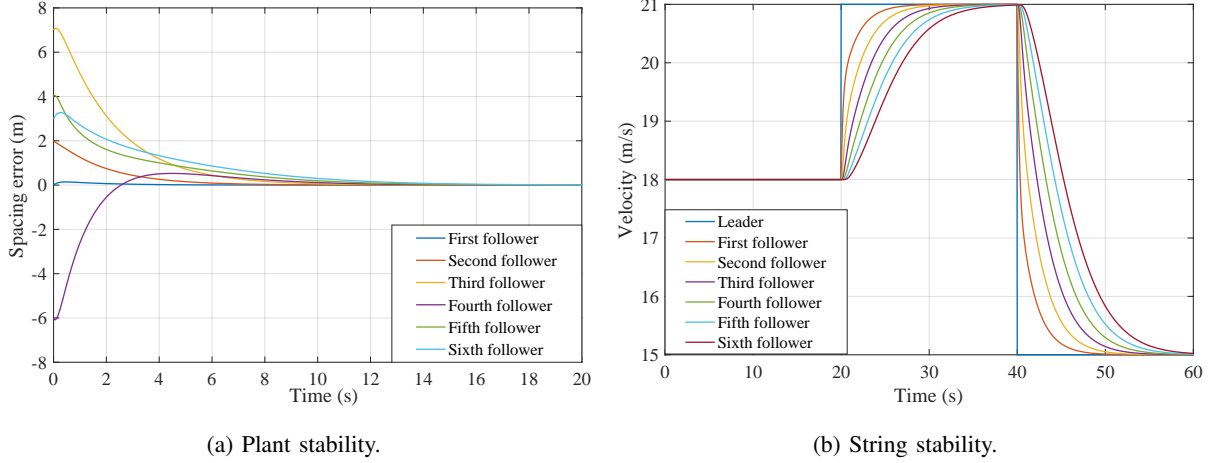


Fig. 5. Control system stability analysis validation.

0.03 vehicle/m. Therefore, we consider the density of transiting non-platoon vehicles on each lane in the range (0.005 vehicle/m, 0.015 vehicle/m). The values of the parameters used for simulations are summarized in Table I.

A. Validation of Theoretical Results

Based on Theorems 1 and 2, we can find that the maximum time delay to guarantee the plant stability and string stability are, respectively, 15.8 ms and 1.1667 s when the control parameters are set to $a_i = 3$ and $b_i = 3, i \in \mathcal{M}$. Hence, we first corroborate our analytical results for both types of stability under the minimum of these two delays, i.e., 15.8 ms. In particular, we model the uncertainty of the wireless system delay between two adjacent vehicles in the platoon system as a time-varying delay in the range (0, 15.8 ms). Vehicles in the platoon are initially assigned different velocities and different inter-vehicle distances. Here, the target velocity is $v_t = 15$ m/s, and the target inter-vehicle distance is $L_t = 20$ m.

Fig. 5(a) shows the time evolution of the velocity errors. We can observe that the spacing error will converge to 0 (a similar result is observed for the velocity error but is omitted due to space limitations). Thus, by choosing the maximum time delay derived from Theorems 1 and 2, we can ensure the plant stability for the platoon system. Next, to verify the string stability, we add disturbances to the leader, that increase the velocity from 18 to 21 m/s at $t = 20$ s and decrease it from 21 to 15 m/s at $t = 40$ s. Note that the disturbance might come from changes of road conditions or malfunctions of the control system. As shown in Fig. 5(b), the velocity error is not amplified when propagating across the platoon, guaranteeing the string stability. In particular, when the velocity of the leader jumps from 18 to 21 m/s, the velocity curve of the sixth follower is more smooth compared with the counterpart of the first follower. Clearly,

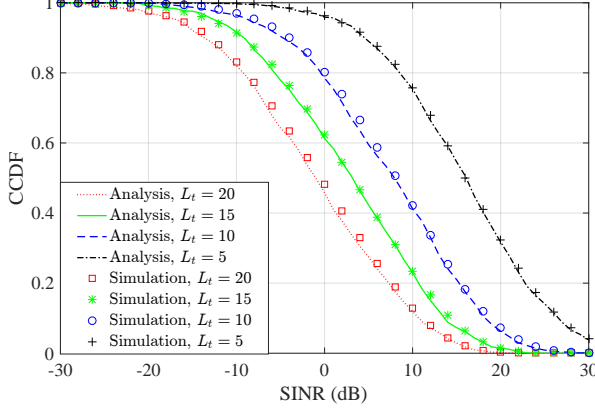


Fig. 6. Validation for the SINR CCDF (22) derived in Theorem 3.

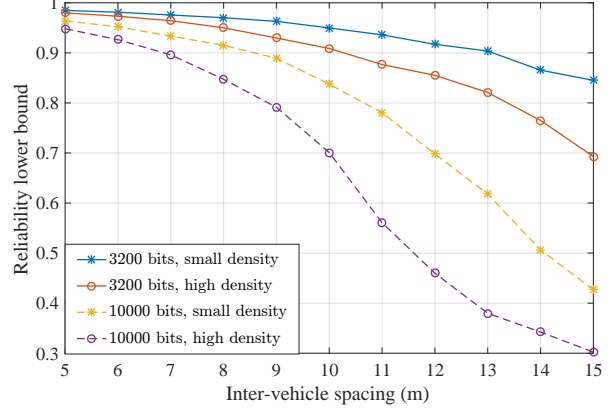


Fig. 7. Reliability lower bound for platoons with different density for non-platoon vehicles and packet sizes.

the delay thresholds, found by Theorems 1 and 2, can guarantee the plant stability and string stability for the platoon system.

Fig. 6 shows the CCDFs in (22) of the SINR derived in Theorem 3 for platoons with different spacings between two consecutive platoon vehicles. Here, to characterize the density difference between overtaking lanes and slow lanes, we assume the vehicle density to be $\lambda_1 = 0.01$ vehicle/m, $\lambda_2 = 0.005$ vehicle/m, $\lambda_3 = 0.005$ vehicle/m, $\lambda_4^{(1)} = 0.01$ vehicle/m, and $\lambda_4^{(2)} = 0.01$ vehicle/m. As observed from Fig. 6, the simulation results match the analytical calculations in (22), guaranteeing the effectiveness to derive the mean and variance of the service time based on (22) in Theorem 3. Moreover, Fig. 6 shows that a smaller spacing in the platoon can lead to a higher probability of being at high SINR regions than the one with a larger spacing. For example, when $L_t = 5$ m, the probability that the SINR will be greater than 10 dB is around 0.76, while the counterpart for the platoon with $L_t = 15$ m is around 0.24. This is due to the fact that vehicles in the platoon with smaller spacings can receive a signal with higher strength from the vehicle immediately ahead.

B. Reliability Analysis

In Fig. 7, we first show the reliability performance derived in Theorem 4 for scenarios with different density of transmitting non-platoon vehicles and different packet sizes. We consider two scenarios: the first scenario with small density, i.e., $\lambda_1 = 0.01$ vehicle/m, $\lambda_2 = 0.005$ vehicle/m, $\lambda_3 = 0.005$ vehicle/m, $\lambda_4^{(1)} = 0.01$ vehicle/m, and $\lambda_4^{(2)} = 0.01$ vehicle/m and the second scenario with high density, i.e., $\lambda_1 = 0.015$ vehicle/m, $\lambda_2 = 0.01$ vehicle/m, $\lambda_3 = 0.01$ vehicle/m, $\lambda_4^{(1)} = 0.015$ vehicle/m, and $\lambda_4^{(2)} = 0.015$ vehicle/m. Moreover, we consider two packet sizes, namely, one with 3200 bits and the other with 10000 bits. As observed from Fig. 7, the reliability lower

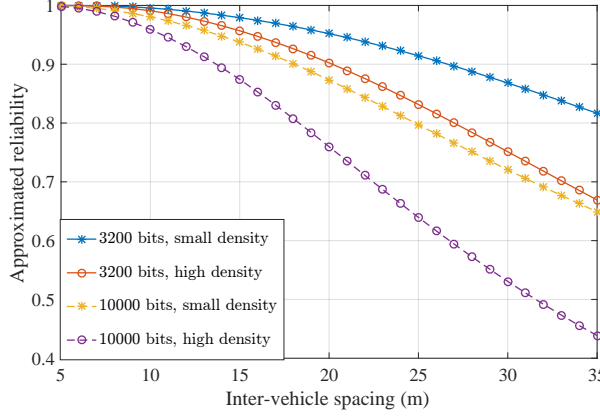


Fig. 8. Approximated reliability for platoons with different density for non-platoon vehicles and packet sizes.

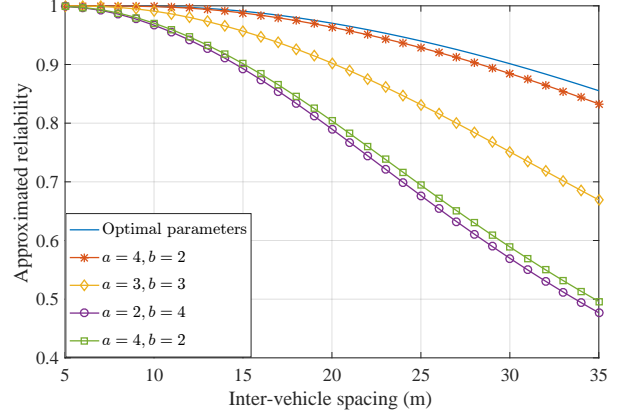


Fig. 9. Optimization design for the control system in Theorem 5.

bounds decrease with the increase of the distance between two consecutive platoon vehicles and the distribution density of transmitting non-platoon vehicles. This is due to the fact that, as the distance or density increases, the SINR will decrease, leading to a decline in data rate and an increase of transmission delay. Also, in Fig. 7, a larger size of packets will lead to an increase of the transmission time and a degradation of the reliability. In addition, from Fig. 7, we can obtain design guidelines on target spacing between two nearby platoon vehicles. That is, in order to ensure that the reliability lower bound of the wireless network exceeds the target threshold, the platoon spacing should be below a typical value. For example, in the scenario with small density of transmitting non-platoon vehicles, the target distance should not be larger than 13 m so that the reliability lower bound can be no less than 0.9 when transmitting small packets. Furthermore, since the target spacing is correlated with the target velocity as shown in (7), we can also have insights about how to choose the target velocity for the platoon system.

Fig. 8 shows the approximated reliability in Corollary 2 for scenarios with different density of vehicles and different packet sizes. The density settings and the packet size are similar to the ones used for Fig. 7. Similar to Fig. 7, we can observe that as the platoon distance increases, the approximated reliability will accordingly decrease. Moreover, the approximated reliability of the platoon in a scenario with lower density of transmitting non-platoon vehicles outperforms the counterpart for the one with high density of transmitting non-platoon vehicles.

Fig. 9 shows the approximated reliability performance under different pairs of control parameters a and b when platoon vehicles are transmitting small packets. In particular, we assume that both a and b are in the range $(2, 4)$. Therefore, by using the optimization results in Theorem 5, we can find the optimal pair of control parameters as $a = 2$ and $b = 2$. As shown in Fig. 9, the

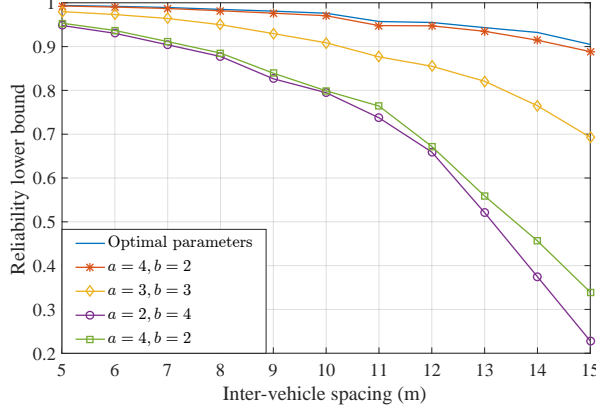


Fig. 10. Optimization design for the control system in Theorem 6.

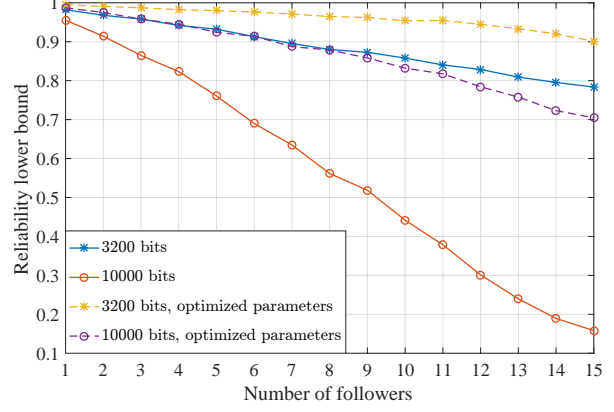


Fig. 11. Reliability for platoons with different number of followers.

platoon with the optimal control parameters outperforms platoons with other control parameters. In particular, compared with the platoon with control parameters $a = 3$ and $b = 3$, the reliability gain of the platoon system with the optimized control parameters can be as much as 25%. In addition, the platoon with the optimal control parameters has more flexibility on the platoon spacing. For example, to achieve a reliability of 0.9, the spacing for the platoon with optimal parameters can be at most 30 m, whereas the spacing for the platoon with $a = 2$ and $b = 4$ cannot exceed 19 m. With more flexibility, the system with the optimal control parameters can tolerate a higher disturbance introduced by rapidly changed road conditions or possible malfunctions of the control system related to the spacing between two consecutive platoon vehicles.

Fig. 10 shows the reliability lower bounds under different control parameters when platoon vehicles are transmitting small packets. Same to the parameter settings in Fig. 9, both a and b are in the range $(2, 4)$. Based on Theorem 6, the optimized parameters are $a = 2$ and $b = 2$, and the performance with optimized parameters is verified in Fig. 10. In particular, the performance gain of choosing the optimized control parameters can be as much as 30%, compared with the platoon with control parameters $a = 3$ and $b = 3$. Comparing Fig. 9 with Fig. 10, we can observe that to achieve the same value of reliability performance, the maximum spacing we can choose when considering the reliability bound would be much smaller than the counterpart when considering approximated reliability. For example, when we consider the approximated reliability, the platoon distance can be as large as 30 m to realize a reliability 0.9. However, when we consider reliability lower bounds, the spacing must be smaller than 15 m, which is half of the spacing selected when considering the approximated reliability. This is due to the fact that when calculating the approximated reliability, we ignore the queuing and processing

delays at the processor and the queuing delay at the transceiver, leading to a much larger spacing threshold.

Fig. 11 shows reliability lower bounds for platoons with different numbers of followers and control parameters. We can observe that, as the number of followers increases, the reliability of the system (Theorem 4) decreases. This stems from the fact that increasing the number of followers reduces the amount of bandwidth assigned for each V2V link in the platoon. As a result, the transmission rate will decrease, and the performance of the wireless network will degrade. Furthermore, according to Fig. 11, we can obtain the design guidelines on how to optimize the number of followers in each platoon to realize a target reliability. For example, when transmitting packets with size 3200 bits, the number of followers should be smaller than 7 so that the reliability lower bound can be no less than 0.9. In addition, from Fig. 11, for different types of packets, we need to choose a proper bandwidth w so as to achieve a satisfactory reliability performance. In this regard, by optimizing the design of the control system, we can increase the number of following vehicles and relax the need for a large bandwidth. In particular, when transmitting small packets, to realize a 0.9 reliability performance, the number of followers in the platoon with optimized control parameters can be at most 15, which is more than twice the one chosen by the platoon with no optimizations on the control system. By allowing more following vehicles in the platoon, the road capacity can further increase, and, thus, improving the traffic situation.

VII. CONCLUSIONS

In this paper, we have proposed an integrated communication and control framework for analyzing the performance and reliability of wirelessly connected vehicular platoons. In particular, we have analyzed plant stability and string stability to derive the maximum wireless system delay that a stable platoon control system can tolerate. In addition, we have derived the end-to-end delay, including queuing, processing, and transmission delay, that a packet will encounter in the wireless communication network by using stochastic geometry and queuing theory. Furthermore, we have conducted theoretical analysis for the reliability of the wireless vehicular platoon, defined as the probability of the wireless network meeting the control systems delay requirements, and derived its lower bounds and approximated expression. Then, we have proposed two optimization mechanisms to select the control parameters for improving the reliability performance of the wireless network in vehicular platoon systems. Simulation results have corroborated the analytical derivations and shown the impact of parameters, such as the density of interfering vehicles,

the packet size, and the platoon size, on the reliability performance of the vehicular platoon. More importantly, the simulation results have shed light on the benefits of integrating control system and wireless network design while providing guidelines to design the platoon system. In particular, the results provide key insights on how to choose the number of followers, the spacing between two consecutive vehicles, and the control parameters for the control system so as to maintain a stable operation for the autonomous platoon.

APPENDIX

A. Proof of Theorem 1

Similar to the consensus problem considered in [40], we use the following candidate Lyapunov function: $V(e) = e^T P e$, where $P = I_{2M \times 2M}$ is a positive definitive matrix. We also assume that there is a continuous nondecreasing function $\psi(x) \geq x$, $x > 0$. Then, the time derivative for $V(e)$ will be:

$$\begin{aligned} \dot{V}(e) = & e^T ((M_1 + M_2) + (M_1 + M_2)^T) e - 2e^T \int_{-\tau(t)}^0 M_2 M_1 e(t+x) dx \\ & - 2e^T \int_{-\tau(t)}^0 M_2 M_2 e(t+x-\tau(t+x)) dx. \end{aligned} \quad (32)$$

Note that for a positive definite matrix ϕ , we have $2v_1^T v_2 \leq v_1^T \phi v_1 + v_2^T \phi^{-1} v_2$. Thus, let $v_1 = -2e^T M_1 M_2$, $\phi = P$, and $v_2 = e(t+x)$. Then, the inequality for the second term of the right-hand side in (32) will be

$$-2e^T \int_{-\tau(t)}^0 M_2 M_1 e(t+x) dx \leq \int_{-\tau(t)}^0 e(t+x)^T e(t+x) dx + \tau(t) e^T M_2 M_1 M_1^T M_2^T e. \quad (33)$$

When $V(e(t+x)) \leq \psi(V(e(t))) = kV(e(t))$ with $k > 1$, $x \in (-\tau(t), 0)$, (33) can be further simplified as: $-2e^T \int_{-\tau(t)}^0 M_2 M_1 e(t+x) dx \leq \tau(t) e^T (M_2 M_1 M_1^T M_2^T + k I_{2N \times 2N}) e$. Similarly, we can perform the same steps for the third term on the right-hand side in (32). Finally, we can obtain $\dot{V}(e) \leq e^T (M_1 + M_2 + (M_1 + M_2)^T + \tau(t) M_2 M_1 M_1^T M_2^T + \tau(t) M_2 M_2 M_2^T M_2^T + 2\tau(t) k I_{2M \times 2M}) e$. Based on the Lyapunov-Razumikhin theorem introduced in [41], if $\dot{V}(e) \leq 0$, i.e., $\tau(t) \leq \lambda_{\min}(-M_1 - M_2 - (M_1 + M_2)^T) / \lambda_{\max}(M_2 M_1 M_1^T M_2^T + M_2 M_2 M_2^T M_2^T + 2k I_{2M \times 2M})$, the system in (6) is asymptotically stable and the augmented error state vector will converge to a zero vector.

B. Proof of Theorem 2

To ensure string stability, the magnitude of the transfer function must satisfy $|T(jf)| \leq 1$, for $f \in \mathbb{R}^+$, where f represents the frequency of sinusoidal excitation signals generated by the leader [42]. The magnitude inequality is equivalent to

$$\Gamma(f) = E f^4 + F f^2 + G \geq 0, \quad (34)$$

where $E = \frac{1}{4}(\tau(t))^2 > 0$, $F = (\frac{1}{4}C^2 - \frac{1}{2}A - \frac{1}{4}B^2)(\tau(t))^2 + 1$, and $G = C^2 - 2A - B^2 - 2AB(\tau(t))$. To solve (34), we need $\Gamma(f') > 0$, where $\frac{d\Gamma(f)}{df}|_{f=f'} = 0$. We can easily find that $\tau(t) \leq \tau_2 = \frac{C^2 - 2A - B^2}{2AB}$.

C. Proof of Lemma 1

$$\begin{aligned}
\mathcal{L}_i^{\text{non-platoon}}(s) &= \mathbb{E}_\Phi \left[\exp \left(-s \sum_{j_1=1}^{n-1} \sum_{c \in \Phi_{j_1}} P_t g_{c,i}(t) (d_{c,i}(t))^{-\alpha} - s \sum_{j_2=n+1}^N \sum_{c \in \Phi_{j_2}} P_t g_{c,i}(t) (d_{c,i}(t))^{-\alpha} \right) \right] \\
&= \mathbb{E}_\Phi \left[\exp \left(-s \sum_{j_1=1}^{n-1} \sum_{c \in \Phi_{j_1}} P_t g_{c,i}(t) (d_{c,i}(t))^{-\alpha} \right) \right] \\
&\quad \times \mathbb{E}_\Phi \left[\exp \left(-s \sum_{j_2=n+1}^N \sum_{c \in \Phi_{j_2}} P_t g_{c,i}(t) (d_{c,i}(t))^{-\alpha} \right) \right] \\
&= \prod_{j_1=1}^{n-1} \mathbb{E}_{\Phi_{j_1}} \left[\prod_{v \in \Phi_{j_1}} \mathbb{E}_{g_{c,i}} \left(\exp \left(-P_t g_{c,i}(t) (d_{c,i}(t))^{-\alpha} \right) \right) \right] \\
&\quad \times \prod_{j_2=n+1}^N \mathbb{E}_{\Phi_{j_2}} \left[\prod_{v \in \Phi_{j_2}} \mathbb{E}_{g_{c,i}} \left(\exp \left(-P_t g_{c,i}(t) (d_{c,i}(t))^{-\alpha} \right) \right) \right] \\
&\stackrel{(a)}{=} \prod_{j_1=1}^{n-1} \mathbb{E}_{\phi_{j_1}} \left[\prod_{v \in \phi_{j_1}} \frac{1}{1 + s P_t d_{v,i}^{-\alpha}} \right] \times \prod_{j_2=n+1}^N \mathbb{E}_{\phi_{j_2}} \left[\prod_{v \in \phi_{j_2}} \frac{1}{1 + s P_t d_{v,i}^{-\alpha}} \right] \\
&\stackrel{(b)}{=} \prod_{j_1=1}^{n-1} \exp \left[-\lambda_{j_1} \int_{(n-j_1)l}^{\infty} \left(1 - \frac{1}{1 + s P_t r^{-\alpha}} \right) \frac{2r}{\sqrt{r^2 - (n-j_1)^2 l^2}} dr \right] \\
&\quad \times \prod_{j_2=n+1}^N \exp \left[-\lambda_{j_2} \int_{(j_2-n)l}^{\infty} \left(1 - \frac{1}{1 + s P_t r^{-\alpha}} \right) \frac{2r}{\sqrt{r^2 - (j_2-n)^2 l^2}} dr \right], \quad (35)
\end{aligned}$$

where (a) follows from the assumption of Rayleigh channel and the channel gain $h_{v,i} \sim \exp(1)$, and in (b), $d_{v,i}$ is replaced with r , and the probability generating function (PGFL) of PPP is utilized [43]. Also, in (b), we leverage the relationship among the distance, the horizontal distance, and the vertical distance.

D. Proof of Theorem 3

Since the fading channel between vehicles $i-1$ and i is a Nakagami channel, $g_{i-1,i}^j$ is a normalized gamma random variable with parameter m . Based on the distribution of $g_{i-1,i}^j$, the CCDF of SINR can be expressed as

$$\mathbb{F}(\theta) = \mathbb{P}(\gamma_{i-1,i}^j > \theta) = \mathbb{P} \left(\frac{P_t g_{i-1,i}^j d_{i-1,i}^{-\alpha}}{\sigma^2 + I_i^{\text{non-platoon}}(t) + I_i^{\text{platoon}}(t)} > \theta \right)$$

$$\begin{aligned}
&= \mathbb{P} \left(g_{i-1,i}^j > \frac{\theta(\sigma^2 + I_i^{\text{non-platoon}}(t) + I_i^{\text{platoon}}(t))}{P_t d_{i-1,i}^{-\alpha}} \right) \\
&\stackrel{(a)}{\approx} 1 - \mathbb{E}_{\Phi \cup \Psi} \left[\left(1 - \exp \left(\frac{-\eta \theta d_{i-1,i}^{\alpha} (\sigma^2 + I_i^{\text{non-platoon}}(t) + I_i^{\text{platoon}}(t))}{P_t} \right) \right)^m \right] \\
&\stackrel{(b)}{=} \sum_{k=1}^m (-1)^{k+1} \binom{m}{k} \mathbb{E}_{\Phi \cup \Psi} \left(\exp \left(\frac{-k \eta \theta d_{i-1,i}^{\alpha} (\sigma^2 + I_i^{\text{non-platoon}}(t) + I_i^{\text{platoon}}(t))}{P_t} \right) \right) \\
&= \sum_{k=1}^m (-1)^{k+1} \binom{m}{k} \exp \left(\frac{-k \eta \theta d_{i-1,i}^{\alpha} \sigma^2}{P_t} \right) \mathbb{E}_{\Phi} \left(\exp \left(\frac{-k \eta \theta d_{i-1,i}^{\alpha} I_i^{\text{non-platoon}}(t)}{P_t} \right) \right) \\
&\quad \mathbb{E}_{\Psi} \left(\exp \left(\frac{-k \eta \theta d_{i-1,i}^{\alpha} I_i^{\text{platoon}}(t)}{P_t} \right) \right) \\
&\stackrel{(c)}{=} \sum_{k=1}^m (-1)^{k+1} \binom{m}{k} \exp \left(\frac{-k \eta \theta d_{i-1,i}^{\alpha} \sigma^2}{P_t} \right) \mathcal{L}_i^{\text{non-platoon}} \left(\frac{k \eta \theta d_{i-1,i}^{\alpha}}{P_t} \right) \mathcal{L}_i^{\text{platoon}} \left(\frac{k \eta \theta d_{i-1,i}^{\alpha}}{P_t} \right), \tag{36}
\end{aligned}$$

where $\eta = m(m!)^{-\frac{1}{m}}$, (a) is based on the approximation of tail probability of a gamma function [44], (b) follows Binomial theorem and the assumption that m is an integer, and the changes in (c) follow the definition of Laplace transform. Also, we can calculate the PDF of the SINR at vehicle i as $f(\theta) = \frac{d(1-\mathbb{F}(\theta))}{d\theta} = -\frac{\mathbb{F}(\theta)}{d\theta}$. Therefore, according to the relationship between the data rate and SINR, we can obtain the mean and variance of service time in (20) and (21).

E. Proof of Theorem 4

The first element in the maximization function is actually a lower bound for the reliability, which is proven by

$$\begin{aligned}
\mathbb{P}(T_1 + T_2 \leq \min(\tau_1, \tau_2)) &= 1 - \mathbb{P}(T_1 + T_2 \geq \min(\tau_1, \tau_2)) \\
&\stackrel{(a)}{\geq} 1 - \frac{\mathbb{E}(T_1 + T_2)}{\min(\tau_1, \tau_2)} = 1 - \frac{\bar{T}_1 + \bar{T}_2}{\min(\tau_1, \tau_2)}, \tag{37}
\end{aligned}$$

where (a) is based on Markov's inequality [45]. For the second element in the maximization function, we leverage the Chernoff bound [46] in (a) to obtain another lower bound. Between these two lower bounds, we can always choose the tighter bound to be closer to the reliability of the wireless network, as shown in (24).

F. Proof of Theorem 5

The Lagrangian of the objective function in the optimization problem is given by

$$\begin{aligned}
\mathcal{F}(a, b, \nu_1, \nu_2, \nu_3, \nu_4, \nu_5, \nu_6) &= \tau - \nu_1(\tau - \min(\tau_1, \tau_2)) - \nu_2(\bar{T}_1 + \bar{T}_2 - \tau) - \\
&\quad \nu_3(a_{\min} - a) - \nu_4(a - a_{\max}) - \nu_5(b_{\min} - b) - \nu_6(b - b_{\max}), \tag{38}
\end{aligned}$$

where $\nu_i \geq 0, 1 \leq i \leq 6$, denotes the Lagrange multiplier associated with constraints in the optimization problem (26)–(28). The dual problem of (26) is thereby expressed as $\mathcal{G}(\nu_1, \nu_2, \nu_3, \nu_4, \nu_5, \nu_6) = \max_{a,b} \mathcal{F}(a, b, \nu_1, \nu_2, \nu_3, \nu_4, \nu_5, \nu_6)$. It can be observed that the problem in (26) is convex with zero duality gap. Therefore, the KKT conditions are both necessary and sufficient for the global optimality of the optimization problem. These conditions are given by:

$$\nu_1 \frac{\partial \min(\tau_1, \tau_2)}{\partial a} + \nu_3 - \nu_4 = 0, \nu_1 \frac{\partial \min(\tau_1, \tau_2)}{\partial b} + \nu_5 - \nu_6 = 0, \quad (39)$$

$$\nu_3(a_{\min} - a) = 0, \nu_4(a - a_{\max}) = 0, \nu_5(b_{\min} - b) = 0, \quad (40)$$

$$\nu_6(b - b_{\max}) = 0, a, b, \nu_1, \nu_2, \nu_3, \nu_4, \nu_5, \nu_6 \geq 0. \quad (41)$$

Based on the conditions (39)–(41), we can obtain the following possible solutions:

- When $\nu_3 = \nu_4 = \nu_5 = \nu_6 = 0$, the optimized control parameters will be a_{opt} and b_{opt} so that $\frac{\partial \min(\tau_1, \tau_2)}{\partial a_{\text{opt}}} = 0$ and $\frac{\partial \min(\tau_1, \tau_2)}{\partial b_{\text{opt}}} = 0$.
- When $\nu_4 = \nu_5 = \nu_6 = 0$ and $\nu_1, \nu_3 \geq 0$, the optimized control parameters will be $a_{\text{opt}} = a_{\min}$ and $b_{\text{opt}} = b'$ as long as $\frac{\partial \min(\tau_1, \tau_2)}{\partial a} \leq 0$ exists for $a_{\min} \leq a \leq a_{\max}$ and $\frac{\partial \min(\tau_1, \tau_2)}{\partial b'} = 0$.
- When $\nu_3 = \nu_5 = \nu_6 = 0$ and $\nu_1, \nu_4 \geq 0$, the optimized control parameters will be $a_{\text{opt}} = a_{\max}$ and $b_{\text{opt}} = b'$ as long as $\frac{\partial \min(\tau_1, \tau_2)}{\partial a} \geq 0$ exists for $a_{\min} \leq a \leq a_{\max}$ and $\frac{\partial \min(\tau_1, \tau_2)}{\partial b'} = 0$.
- When $\nu_3 = \nu_4 = \nu_6 = 0$ and $\nu_1, \nu_5 \geq 0$, the optimized control parameters will be $a_{\text{opt}} = a'$ and $b_{\text{opt}} = b_{\min}$ as long as $\frac{\partial \min(\tau_1, \tau_2)}{\partial a'} = 0$ and $\frac{\partial \min(\tau_1, \tau_2)}{\partial b} \leq 0$ exists for $b_{\min} \leq b \leq b_{\max}$.
- When $\nu_3 = \nu_4 = \nu_5 = 0$ and $\nu_1, \nu_6 \geq 0$, the optimized control parameters will be $a_{\text{opt}} = a'$ and $b_{\text{opt}} = b_{\max}$ as long as $\frac{\partial \min(\tau_1, \tau_2)}{\partial a'} = 0$ and $\frac{\partial \min(\tau_1, \tau_2)}{\partial b} \geq 0$ exists for $b_{\min} \leq b \leq b_{\max}$.
- When $\nu_4 = \nu_6 = 0$ and $\nu_1, \nu_3, \nu_5 > 0$, the optimized control parameters will be $a_{\text{opt}} = a_{\min}$ and $b_{\text{opt}} = b_{\min}$ as long as $\frac{\partial \min(\tau_1, \tau_2)}{\partial a} \leq 0$ and $\frac{\partial \min(\tau_1, \tau_2)}{\partial b} \leq 0$ exists for $a_{\min} \leq a \leq a_{\max}$ and $b_{\min} \leq b \leq b_{\max}$.
- When $\nu_4 = \nu_5 = 0$ and $\nu_1, \nu_3, \nu_6 > 0$, the optimized control parameters will be $a_{\text{opt}} = a_{\min}$ and $b_{\text{opt}} = b_{\max}$ as long as $\frac{\partial \min(\tau_1, \tau_2)}{\partial a} \leq 0$ and $\frac{\partial \min(\tau_1, \tau_2)}{\partial b} \geq 0$ exists for $a_{\min} \leq a \leq a_{\max}$ and $b_{\min} \leq b \leq b_{\max}$.
- When $\nu_3 = \nu_6 = 0$ and $\nu_1, \nu_4, \nu_5 > 0$, the optimized control parameters will be $a_{\text{opt}} = a_{\max}$ and $b_{\text{opt}} = b_{\min}$ as long as $\frac{\partial \min(\tau_1, \tau_2)}{\partial a} \geq 0$ and $\frac{\partial \min(\tau_1, \tau_2)}{\partial b} \leq 0$ exists for $a_{\min} \leq a \leq a_{\max}$ and $b_{\min} \leq b \leq b_{\max}$.
- When $\nu_3 = \nu_6 = 0$ and $\nu_1, \nu_4, \nu_5 > 0$, the optimized control parameters will be $a_{\text{opt}} = a_{\max}$ and $b_{\text{opt}} = b_{\max}$ as long as $\frac{\partial \min(\tau_1, \tau_2)}{\partial a} \geq 0$ and $\frac{\partial \min(\tau_1, \tau_2)}{\partial b} \geq 0$ exists for $a_{\min} \leq a \leq a_{\max}$ and $b_{\min} \leq b \leq b_{\max}$.

G. Proof of Theorem 6

To prove theorem 6, we first let $\tau_3 = \frac{\bar{T}_1 + \bar{T}_2}{\min(\tau_1, \tau_2)}$, $0 \leq \tau_3 \leq 1$, and the two functions in the (29) can be simplified as

$$1 - \frac{\bar{T}_1 + \bar{T}_2}{\min(\tau_1, \tau_2)} = 1 - \tau_3, \quad (42)$$

$$1 - \exp\left(\bar{T}_1 + \bar{T}_2 - \min(\tau_1, \tau_2) \ln\left(\frac{\min(\tau_1, \tau_2)}{\bar{T}_1 + \bar{T}_2}\right)\right) = 1 - \exp\left[(\bar{T}_1 + \bar{T}_2) \left(1 - \frac{1}{\tau_3} \ln\left(\frac{1}{\tau_3}\right)\right)\right], \quad (43)$$

where both (42) and (43) are decreasing functions in terms of τ_3 . Note that finding the maximum value between functions (42) and (43) is equivalent to maximizing the maximal value of (42) and (43). Therefore, the solution for (29)–(31) is to minimize τ_3 , which equals to maximizing $\min(\tau_1, \tau_2)$. In other words, the solutions for the optimization problem in (26)–(28) apply to the problem in (29)–(31) as long as the solutions can guarantee $\bar{T}_1 + \bar{T}_2 \leq \min(\tau_1, \tau_2)$.

REFERENCES

- [1] T. Zeng, O. Semiari, W. Saad, and M. Bennis, “Integrated communications and control co-design for vehicular platoon systems,” in *Proc. of IEEE International Conference on Communication (ICC)*, Kansas City, MO, USA, May 2018.
- [2] A. Ferdowsi, U. Challita, and W. Saad, “Deep learning for reliable mobile edge analytics in intelligent transportation systems,” *arXiv preprint arXiv:1712.04135*, 2017.
- [3] R. Hall and C. Chin, “Vehicle sorting for platoon formation: Impacts on highway entry and throughput,” *Transportation Research Part C: Emerging Technologies*, vol. 13, no. 5-6, pp. 405–420, Oct.–Dec. 2005.
- [4] K.-Y. Liang, J. Mårtensson, and K. H. Johansson, “Heavy-duty vehicle platoon formation for fuel efficiency,” *IEEE Transactions on Intelligent Transportation Systems*, vol. 17, no. 4, pp. 1051–1061, Apr. 2016.
- [5] C. Nowakowski, J. O’Connell, S. E. Shladover, and D. Cody, “Cooperative adaptive cruise control: Driver acceptance of following gap settings less than one second,” in *Proc. of the Human Factors and Ergonomics Society Annual Meeting*, Los Angeles, CA, USA, Sept. 2010.
- [6] C. Perfecto, J. Del Ser, and M. Bennis, “Millimeter-wave V2V communications: Distributed association and beam alignment,” *IEEE Journal on Selected Areas in Communications*, vol. 35, no. 9, pp. 2148–2162, Sept. 2017.
- [7] I. G. Jin, S. S. Avedisov, and G. Orosz, “Stability of connected vehicle platoons with delayed acceleration feedback,” in *Proc. of ASME Dynamic Systems and Control Conference*, Stanford, CA, USA, Oct. 2013.
- [8] C. Bergenhem, S. Shladover, E. Coelingh, C. Englund, and S. Tsugawa, “Overview of platooning systems,” in *Proc. of ITS World Congress*, Vienna, Austria, Oct. 2012.
- [9] X. Liu, A. Goldsmith, S. S. Mahal, and J. K. Hedrick, “Effects of communication delay on string stability in vehicle platoons,” in *Proc. of Intelligent Transportation Systems*, Oakland, CA, USA, Aug. 2001.
- [10] H. Peng, D. Li, Q. Ye, K. Abboud, H. Zhao, W. Zhuang, and X. S. Shen, “Resource allocation for D2D-enabled inter-vehicle communications in multiplatoons,” in *Proc. of IEEE International Conference on Communications (ICC)*, Paris, France, May 2017.
- [11] P. S. Bithas, A. G. Kanatas, D. B. da Costa, P. K. Upadhyay, and U. S. Dias, “On the double-generalized gamma statistics and their application to the performance analysis of v2v communications,” *IEEE Transactions on Communications*, vol. 66, no. 1, pp. 448–460, Jan. 2018.
- [12] P. S. Bithas, A. G. Kanatas, D. B. da Costa, and P. K. Upadhyay, “Transmit antenna selection in vehicle-to-vehicle time-varying fading channels,” in *Proc. of IEEE International Conference on Communications (ICC)*, Paris, France, May 2017.
- [13] X. Du, H. Zhang, H. Van Nguyen, and Z. Han, “Stacked lstm deep learning model for traffic prediction in vehicle-to-vehicle communication,” in *Proc. of IEEE Vehicular Technology Conference (VTC-Fall)*, Toronto, Canada, Sept. 2017.
- [14] V. V. Chetlur and H. S. Dhillon, “Coverage analysis of a vehicular network modeled as Cox process driven by Poisson line process,” *arXiv preprint arXiv:1709.08577*, 2017.
- [15] H. Peng, D. Li, K. Abboud, H. Zhou, H. Zhao, W. Zhuang, and X. S. Shen, “Performance analysis of IEEE 802.11 p DCF for multiplatooning communications with autonomous vehicles,” *IEEE Transactions on Vehicular Technology*, vol. 66, no. 3, pp. 2485–2498, Mar. 2017.

- [16] Y. Hu, H. Li, Z. Chang, R. Hou, and Z. Han, "End-to-end backlog and delay bound analysis using martingale for internet of vehicles," in *Proc. of IEEE Conference on Standards for Communications and Networking (CSCN)*, Helsinki, Finland, Sept. 2017.
- [17] R. Kaewpuang, D. Niyato, P.-S. Tan, and P. Wang, "Cooperative management in full-truckload and less-than-truckload vehicle system," *IEEE Transactions on Vehicular Technology*, vol. 66, no. 7, pp. 5707–5722, Jul. 2017.
- [18] A. Vahidi and A. Eskandarian, "Research advances in intelligent collision avoidance and adaptive cruise control," *IEEE transactions on intelligent transportation systems*, vol. 4, no. 3, pp. 143–153, Sept. 2003.
- [19] K. Li and P. Ioannou, "Modeling of traffic flow of automated vehicles," *IEEE Transactions on Intelligent Transportation Systems*, vol. 5, no. 2, pp. 99–113, Jun. 2004.
- [20] G. Orosz, "Connected cruise control: modelling, delay effects, and nonlinear behaviour," *Vehicle System Dynamics*, vol. 54, no. 8, pp. 1147–1176, Aug. 2016.
- [21] Z. Gong and M. Haenggi, "Interference and outage in mobile random networks: Expectation, distribution, and correlation," *IEEE Transactions on Mobile Computing*, vol. 13, no. 2, pp. 337–349, Feb. 2014.
- [22] R. He, A. F. Molisch, F. Tufvesson, Z. Zhong, B. Ai, and T. Zhang, "Vehicle-to-vehicle propagation models with large vehicle obstructions," *IEEE Transactions on Intelligent Transportation Systems*, vol. 15, no. 5, pp. 2237–2248, Oct. 2014.
- [23] G. Acosta-Marum and M. Ingram, "Doubly selective vehicle-to-vehicle channel measurements and modeling at 5.9 GHz," in *Proc. International Symposium Wireless Personal Multimedia Communication*, San Diego, CA, USA, Sept. 2006.
- [24] M. Bando, K. Hasebe, A. Nakayama, A. Shibata, and Y. Sugiyama, "Dynamical model of traffic congestion and numerical simulation," *Physical review E*, vol. 51, no. 2, p. 1035, Feb. 1995.
- [25] J. Ploeg, E. Semsar-Kazerooni, G. Lijster, N. van de Wouw, and H. Nijmeijer, "Graceful degradation of cooperative adaptive cruise control," *IEEE Transactions on Intelligent Transportation Systems*, vol. 16, no. 1, pp. 488–497, Feb. 2015.
- [26] G. A. Baker, *Essentials of Padé approximants*. Academic Press, 1975.
- [27] I. G. Jin and G. Orosz, "Dynamics of connected vehicle systems with delayed acceleration feedback," *Transportation Research Part C: Emerging Technologies*, vol. 46, pp. 46–64, Sept. 2014.
- [28] Y. Yang, M. Shao, S. Zhu, B. Ugaonkar, and G. Cao, "Towards event source unobservability with minimum network traffic in sensor networks," in *Proc. of ACM conference on Wireless network security*, Alexandria, VA, USA, Mar. 2008.
- [29] L. Kleinrock, *Queueing systems, volume 1: Theory*. Wiley New York, 1976.
- [30] D. Puccinelli and M. Haenggi, "Wireless sensor networks: applications and challenges of ubiquitous sensing," *IEEE Circuits and systems magazine*, vol. 5, no. 3, pp. 19–31, Sept. 2005.
- [31] P. J. Burke, "The output of a queueing system," *Operations research*, vol. 4, no. 6, pp. 699–704, Dec. 1956.
- [32] P. G. Harrison and N. M. Patel, *Performance modelling of communication networks and computer architectures*. Addison-Wesley Longman Publishing Co., Inc., 1992.
- [33] Z. Bai, J. Demmel, J. Dongarra, A. Ruhe, and H. van der Vorst, *Templates for the solution of algebraic eigenvalue problems: a practical guide*. SIAM, 2000.
- [34] X. Ma, X. Chen, and H. H. Refai, "Performance and reliability of dsrc vehicular safety communication: a formal analysis," *EURASIP Journal on Wireless Communications and Networking*, vol. 2009, no. 1, pp. 1–13, Jan. 2009.
- [35] J. Prados-Garzon, J. J. Ramos-Munoz, P. Ameigeiras, P. Andres-Maldonado, and J. M. Lopez-Soler, "Modeling and dimensioning of a virtualized mme for 5G mobile networks," *IEEE Transactions on Vehicular Technology*, vol. 66, no. 5, pp. 4383–4395, May 2017.
- [36] Radar sensing for driverless vehicles. [Online]. Available: <https://www.digikey.com/en/articles/techzone/2016/nov/radar-sensing-for-driverless-vehicles>
- [37] J. B. Kenney, "Dedicated short-range communications (DSRC) standards in the United States," *Proceedings of the IEEE*, vol. 99, no. 7, pp. 1162–1182, Jul. 2011.
- [38] Berkeley highway lab website. [Online]. Available: <http://bhl.path.berkeley.edu>
- [39] S. Panichpapiboon and L. Cheng, "Irresponsible forwarding under real intervehicle spacing distributions," *IEEE Transactions on Vehicular Technology*, vol. 62, no. 5, pp. 2264–2272, Jun. 2013.
- [40] K. Liu, G. Xie, and L. Wang, "Consensus for multi-agent systems under double integrator dynamics with time-varying communication delays," *International Journal of Robust and Nonlinear Control*, vol. 22, no. 17, pp. 1881–1898, Sept. 2011.
- [41] J. K. Hale and S. M. V. Lunel, *Introduction to functional differential equations*. Springer Science & Business Media, 2013, vol. 99.
- [42] D. Swaroop and J. K. Hedrick, "String stability of interconnected systems," *IEEE Transactions on Automatic Control*, vol. 41, no. 3, pp. 349–357, Mar. 1996.
- [43] M. Haenggi, *Stochastic geometry for wireless networks*. Cambridge University Press, 2012.
- [44] T. Bai and R. W. Heath, "Coverage and rate analysis for millimeter-wave cellular networks," *IEEE Transactions on Wireless Communications*, vol. 14, no. 2, pp. 1100–1114, Feb. 2015.
- [45] E. M. Stein and R. Shakarchi, *Real analysis: measure theory, integration, and Hilbert spaces*. Princeton University Press, 2009.
- [46] W. Hoeffding, "Probability inequalities for sums of bounded random variables," *Journal of the American statistical association*, vol. 58, no. 301, pp. 13–30, Mar. 1963.